

# An LS-DYNA material model for simulations of hot stamping processes of ultra high strength steels

Dr. Tobias Olsson

Engineering Research Nordic AB,

Linköping, Sweden

## Summary:

This paper presents a new material model (\*MAT\_244) in LS-DYNA capable of simulating phase transition during quenching and forming. Usually during forming the blank is initially heated to become fully austenitized and then continuously formed and cooled. When the temperature is decreasing the austenite decomposes into different product phases. The amount of each phase does not only depend on the mechanical history, but also on the cooling rate of the blank. A higher cooling rate increases the amount of the harder phases (bainite and martensite) whereas a slow process gives higher content of ferrite and pearlite.

This thermo-elastoplastic model is based on the isotropic von-Mises yield criterion with an associated plastic flow rule. It includes both the decomposition of austenite into ferrite, pearlite, bainite and martensite, and transformation plasticity.

The examples show that the model is well suited for hot stamping simulations and it should be possible to simulate different steel compositions at different cooling rates to obtain a good prediction of the hardening process and the properties of the final product.

## Keywords:

Material models, phase transitions, hot stamping, forming

## 1 Introduction

The use of ultra high strength (UHS) steels is becoming more and more popular in applications where strength and weight are important factors. These steels are used for strengthen crucial parts in new vehicles, for example, by the automotive and aeronautical industries. To achieve these material properties one usually heats the steel above the austenization temperature (for example 1200 K) and by cooling at higher and lower rates the steel undergoes different phase transformations. It is the cooling path together with the deformation during the forming (plastic strains) that governs the final properties of the steel product. To be able to accurately describe the plastic flow during phase transformations it is necessarily to include the TRIP phenomenon. TRIP stands for Transformation Induced Plasticity and is the irreversible strain that occurs at stresses below the actual yield point of the current phase.

The new material model (\*MAT\_UHS\_STEEL) in LS-DYNA [1] is based on, but not restricted to the work done by Åkerström [2] and includes four optional phase-transformations: austenite—ferrite, austenite—pearlite, austenite—bainite and austenite—martensite.

The complete model is quite computing intense with all phase transitions active. Therefore it is also possible to use it as a simplified version for example in crash simulations. In this simpler version the state of the steel is inherited from the forming simulations by using a so called *dynain* file. With this option it is possible to use properties from the inhomogeneous newly formed steel. That includes the final composition of the steel and the current yield limit, for each element in the model.

## 2 Theoretical framework

The material is based on hypoelasticity and the stress rates are given by Hooke's generalised law. That is, the rate  $\dot{\sigma}_{ij}$  is given by

$$\dot{\sigma}_{ij} = \left( C_{ijkl} \dot{\varepsilon}_{kl}^e \right) = C_{ijkl} \left( \dot{\varepsilon}_{kl} - \dot{\varepsilon}_{kl}^p \right) + \dot{C}_{ijkl} \left( \varepsilon_{kl} - \varepsilon_{kl}^p \right)$$

where  $\varepsilon_{kl}^e$  represents the elastic strain,  $C_{ijkl}$  is the elastic stiffness,  $\varepsilon_{kl}^p$  is the plastic strain and  $\varepsilon_{kl}$  is the total strain. The rate formulation of the elastic stiffness is included due to the optional temperature-time dependency of Young's modulus. In associated plasticity the plastic flow is orthogonal to the yield surface  $y(\sigma_{ij}, \bar{\varepsilon}_1^p, \dots, \bar{\varepsilon}_5^p) = 0$ . The yield function is expressed as

$$y = \bar{\sigma} - \sigma_y(\bar{\varepsilon}_1^p, \dots, \bar{\varepsilon}_5^p)$$

where  $\bar{\sigma}$  is the effective stress and  $\sigma_y$  is the total hardening function. In this model with five phases the total hardening function is composed by a mixture of the five phases

$$\sigma_y = x_1 \sigma_1^y(\bar{\varepsilon}_1^p) + \dots + x_5 \sigma_5^y(\bar{\varepsilon}_5^p)$$

where  $x_i$  is the true volumetric fraction of the phase  $i$  and  $\sigma_i^y$  is the hardening function for phase  $i$ . If the effective stress reaches the yield stress the material undergoes plastic deformation as an ordinary von Mises material. However, if the effective stress is less than the yield stress and phase transformations have begun it is still possible to have plastic deformations. These plastic deformations that occur below the yield stress are due to the transformation induced plasticity (TRIP) and are explained in more detail below.

### 2.1 Austenite decomposition model

The decomposition model used is based on the model described in the work by Kirkaldy and Venugopalan [3] with enhancements by Leblond [4] and Watt et al. [5]. The application to boron steel is taken from Åkerström et al. [6], Åkerström and Oldenburg [7], and Åkerström [2]. Kirkaldy and Venugopalan [3] introduced a weighted variable which they call the ghost fraction,  $X$ . The ghost fraction is defined as the instantaneous amount divided by the equilibrium amount, such that the ghost fraction varies between  $0 < X < 1$ , and tends to 1 at equilibrium. Following Åkerström and Oldenburg [7] and Li et al. [8] the rate equations for describing the phases between austenite and martensite (ferrite, pearlite and bainite) can be written using these ghost fractions as

$$\dot{X}_k = g_k(G) f_k(X_k) h_k(C) i_k(T - T_k), \quad k = 2, 3, 4$$

where the value of the constant  $k$  means ferrite, pearlite, and bainite, respectively and  $g_k(G)$  is a function dependent on the grain size number of the austenite defined by the American Society for Testing and Materials (ASTM). The function  $h_k(C)$  is a weight factor for the actual phase  $k$ . It depends on the chemical composition of the material. The temperature influence is given by  $i_k(T - T_k)$  where  $T$  is the absolute temperature and  $T_k$  is the activation temperature for phase  $k$ . The activation temperatures for the different reactions can be used directly if they are found during experiments. On the other hand if no such data is available the undercooling temperatures are calculated based on the work done by Watt et al. [5]. Finally,  $f_k(X_k)$  is a function dependent on the current amount of phase  $k$  and for the ferrite, pearlite and bainite reaction the function reads

$$f_i(X_i) = X_i^{a(X_i-1)} (1 - X_i)^{aX_i}, \quad i = 2, 3, 4$$

where  $a$  is a material parameter. The decomposition of austenite into martensite is described by

$$x_5 = x_1 \left( 1 - e^{-\alpha(T_5 - T)} \right)$$

where the lower case denote the true volume fraction of the martensite and austenite respectively,  $\alpha$  is a material dependent constant and  $T_5$  is the starting temperature for the martensite phase.

### 3 Examples

#### 3.1 Example 1: Numisheet 2008 benchmark 3

The first example is taken from the Numisheet 2008 benchmark 3 test. The benchmark is based on continuous press hardening of a boron alloyed steel, in this case a b-pillar. The material used in the simulation is a 22MnB5 alloy with thickness 1.95 mm. The material parameters are taken from the benchmark test and input data from the hardening phases were taken from Sjöström [9]. The result after forming and quenching of the specimen show where the quenching process may have difficulties due to not sufficient cooling rate (contact between the tools and the b-pillar). Figure 1 below shows the (Vicker-) hardness (VH) calculated by the model. The variation is due to the amount of martensite in after the quenching process. Figure 2 show the plastic strain at the weaker part (less HV) of the b-pillar and the necking is clearly captured. In Figure 3 the sheet thickness for section 3a is visualized and compared to the experiment. The simulated thickness corresponds very well to the Numisheet 2008 benchmark 3 test.

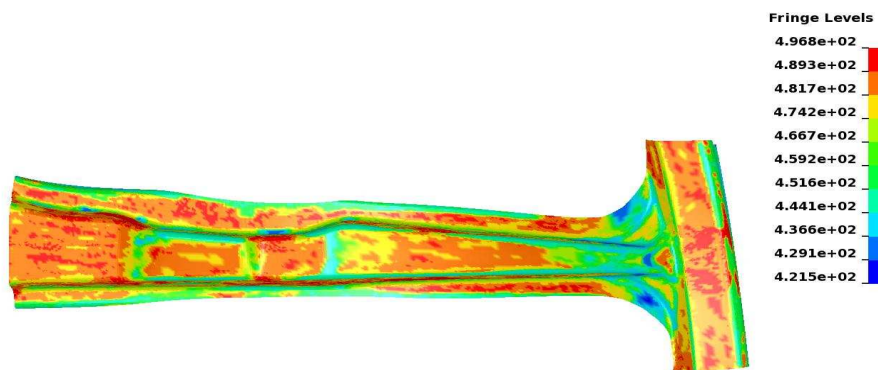


Figure 1: Vickers hardness after quenching the b-pillar. Maximum value = 496.

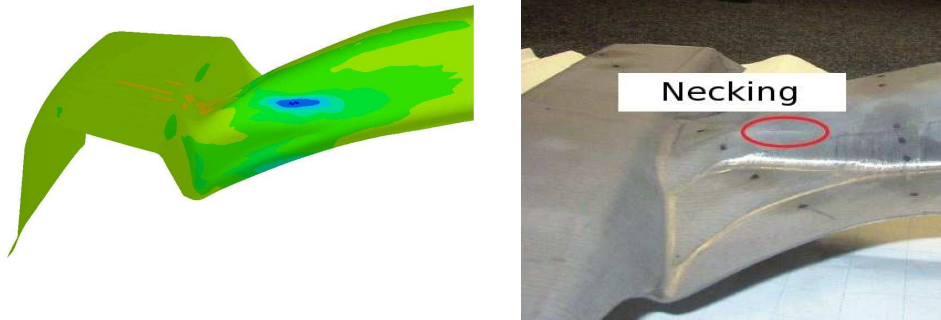


Figure 2: Plastic strains after quenching (left) and a photo from the experiment that shows the necking phenomena (right).

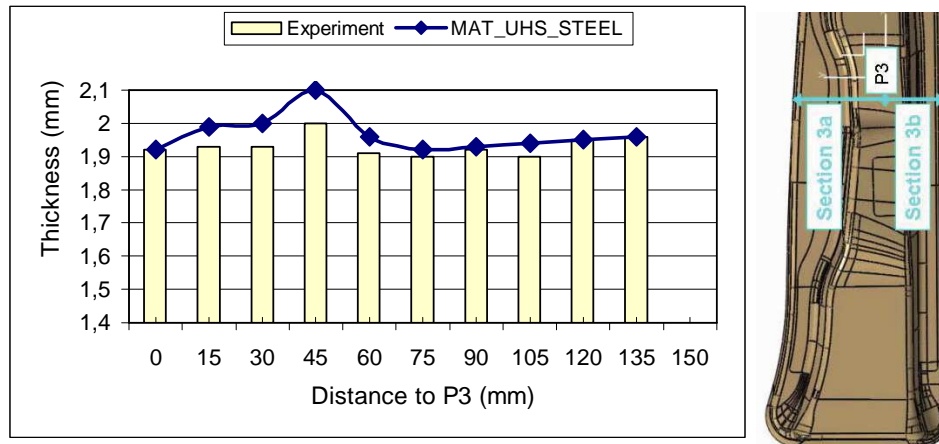


Figure 3: (Left) Experimental result: Sheet thickness section 3a. (Right) Section 3a and the point P3 visualized

### 3.2 Example 2: Cooling of a 8 mm sheet

A cooling example taken from the hot rolling line from SSAB Borlänge/Sweden will show the phase distribution through the thickness of the 8 mm sheet. The sheet is a 1010-like steel, it was heated to approximately 1146 K and assumed to be fully austenitized. The cooling was done with 20 C water in 6+2 curtains (the last two curtains are grouped together as one in the simulation). This simple model is composed of 216 (6x6x6) brick elements and the cooling (water) is applied to the top surface.

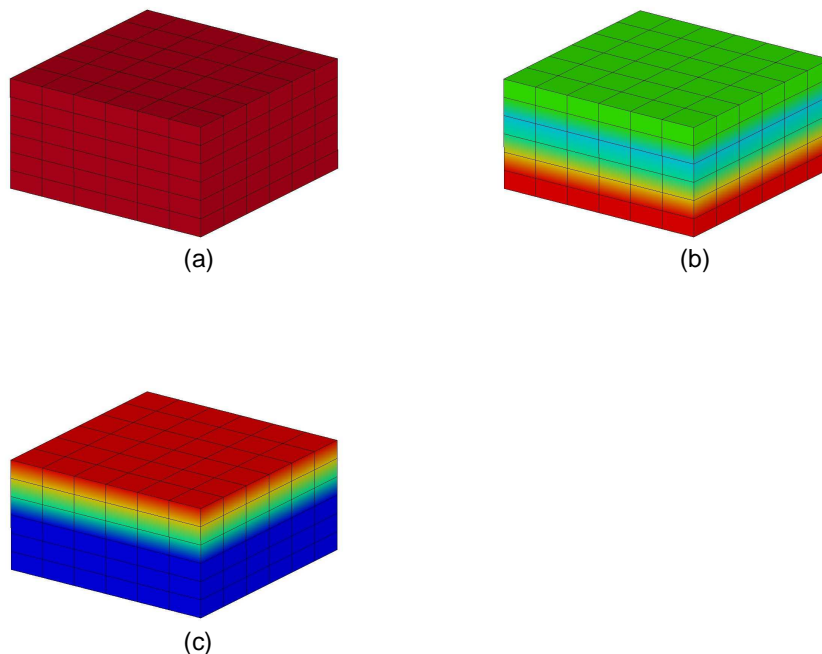


Figure 4: (a) Initial state with 100 % austenite and a temperature of 1146 K; (b) Amount ferrite 28 % - 31 % at the final temperature 934 K; (c) Amount pearlite 4 % - 5 % at the final temperature 934 K.

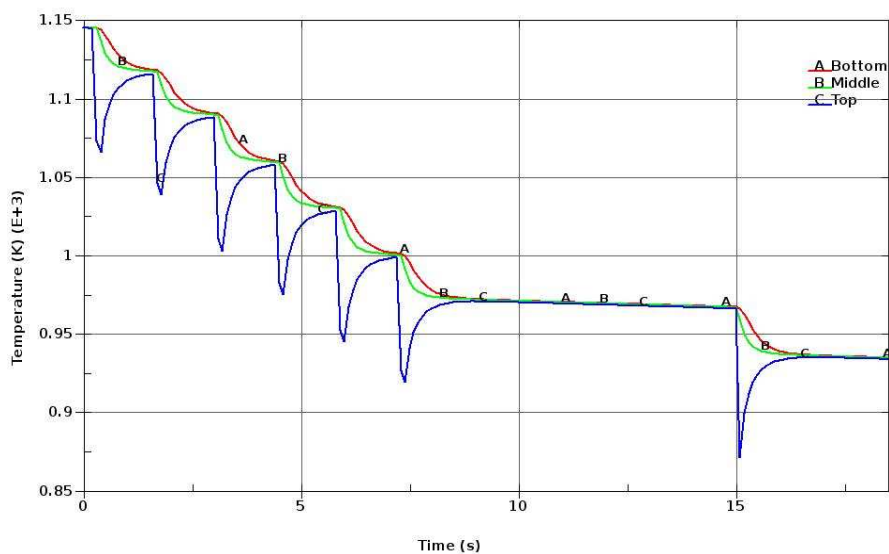


Figure 5: Final temperature 934 K; Temperature history A = Bottom surface, B = Middle surface and C = Top surface

The result after the cooling simulation is shown in Figure 4. After the last water curtain the simulation is stopped so the final cooling to room temperature is not included. During the 8 showers the temperature has dropped from 1146 K down to 934 K and phase transition is initiated. Figure 4(a) shows the initial state with the start temperature 1146 K. In Figure 4(b) and 4(c) the final volume fractions of ferrite (28 % - 31 %) and pearlite (4 % - 5 %) are shown. The temperature is still too high for the bainite phase and martensite phase to be initiated. In Figure 5 the temperature history is given for the top, middle and lower surface and the final temperature goes down to 934 K. The water curtains are clearly visible and the temperature drops quickly when water is applied. In Table 1 the simulation is compared with data, given by MEFOS, directly after the last water shower. The experiment was done at SSAB Borlänge/Sweden. The simple model used in this example compares surprisingly well with the experiment. The temperature after the last shower is only 9 degrees to low. The thermal data for the steel were taken from a 1010 steel and may not be accurate enough. This can explain the difference between the amount of ferrite and pearlite given in table 1.

Table 1: Comparison between experimental data and simulation. The values are taken from experiment done at SSAB Borlänge/Sweden and are measured directly after the last water shower

	Final Temp	Ferrite	Pearlite	Bainite	Martensite
1010-STEEL	943 K	18-36 %	0-12 %	0 %	0 %
MAT_UHS_STEEL	934 K	28-31 %	4-5 %	0 %	0 %

## 4 Conclusions

It is shown that the material model \*MAT\_UHS\_STEEL (\*MAT\_244) in LS-DYNA [1] is capable of simulating the hot forming and hardening both for shell and solid models. In addition to standard responses, it is also possible to obtain the phase composition. The validation against the Numisheet 2008 benchmark 3 test shows a very fine agreement and in the cooling example the results compares well with the experiment.

## Acknowledgement

The experimental material data and help in Example 2 were given by the Metallurgical Research Institute AB (MEFOS), Luleå, Sweden and are gratefully appreciated.

## 5 Literature

- [1] Hallqvist J.O., LS-DYNA Keyword manual v 971, Livermore Software Technology Corporation, Livermore, California.
- [2] Åkerström P.: Modelling and simulation of hot stamping, PhD dissertation LTU-DT-06/30-SE, Luleå University of Technology, Luleå, Sweden 2006.
- [3] Kikaldy, J. S. and Venugoplan D., Prediction of microstructure and hardenability in low alloy steels, In: *Phase Transformations in Ferrite Alloys, Philadelphia*, Eds. Marder A. R. and Goldstein J. I., 1983.
- [4] Leblond J. B., Devaux J. and Devaux J. C., Mathematical modelling of transformation plasticity in steels I: case of ideal-plastic phases, *International Journal of Plasticity*, 5, 1989, 551-572.
- [5] Watt D. F., Coon L., Bibby M., Goldack J. and Henwood C., An algorithm for modelling microstructural development in weld heat-affected zones (part A) reaction kinetics, *Acta Metallurgica*, 36, 1988, 3029-3035.
- [6] Åkerström P., Bergman G. and Oldenburg M., Numerical implementation of a constitutive model for simulation of hot stamping, *Modelling and Simulation in Materials Science and Engineering*, 15, 2007, 105-119.
- [7] Åkerström P. and Oldenburg M., Austenite decomposition during press hardening of a boron steel --- Computer simulation and test, *Journal of Materials Processing Technology*, 174, 2006, 399-406.
- [8] Li M. V., Niebuhr D. V., Meekisho L. L. and Atteridge D. G., A computational model for the prediction of steel hardenability, *Metallurgical and Materials transactions B*, 29, 1998, 661-672.
- [9] Sjöström S., The calculation of quench stresses in steel, Ph.D. Dissertation No. 84, Linköping University, Linköping, Sweden 1982.